Chapter 6

ENSO, ATLANTIC CLIMATE VARIABILITY, AND THE WALKER AND HADLEY CIRCULATIONS

Chunzai Wang
NOAA Atlantic Oceanographic and Meteorological Laboratory, 4301 Rickenbacker Causeway, Miami, Florida 33149, U.S.A.
E-mail: Chunzai.Wang@noaa.gov.

Abstract

This chapter describes and discusses the Walker and Hadley circulations associated with the El Niño/Southern Oscillation (ENSO), the Atlantic "Niño", the tropical Atlantic meridional gradient variability, the Western Hemisphere warm pool (WHWP), and the North Atlantic Oscillation (NAO). During the warm phase of ENSO, the Pacific Walker circulation, the western Pacific Hadley circulation, and the Atlantic Hadley circulation are observed to be weakened, whereas the eastern Pacific Hadley circulation is strengthened. During the peak phase of the Atlantic Niño, the Atlantic Walker circulation weakens and extends eastward and the Atlantic Hadley circulation strengthens. The tropical Atlantic meridional gradient variability corresponds to a meridional circulation in which the air rises over the warm sea surface temperature (SST) anomaly region, flows toward the cold SST anomaly region aloft, sinks in the cold SST anomaly region, then crosses the equator toward the warm SST region in the lower troposphere. During periods when the NAO index is high, the atmospheric Ferrel and Hadley circulations are strengthened, consistent with surface westerly and easterly wind anomalies in the North Atlantic and in the middle to tropical Atlantic, respectively. The chapter also discusses a tropospheric bridge by the Walker/Hadley circulation that links the Pacific El Niño with warming of the tropical North Atlantic (TNA) and the WHWP.

H.F. Diaz and R.S. Bradley (eds.), The Hadley Circulation: Present, Past and Future, 173–202.

1. INTRODUCTION

Pacific and Atlantic climate phenomena include the El Niño/Southern Oscillation (ENSO), the Atlantic "Niño", the tropical Atlantic meridional gradient variability, the Western Hemisphere warm pool (WHWP), and the North Atlantic Oscillation (NAO). All have unique variations in time that impact Western Hemisphere climate and that are interlinked (or not) in various ways. The warm phase of ENSO, El Niño, shows positive sea surface temperature (SST) anomalies in the central/eastern equatorial Pacific and an east-west seesaw in the tropical sea level pressure (SLP) between the Western and Eastern Hemispheres (see ENSO overviews by Philander [1990] and Neelin et al. [1998]). ENSO alters the sources of atmospheric heating, which then affect atmospheric circulation and climate on a global scale (e.g., Oort and Yienger 1996; Klein et al. 1999; Wang 2002a).

An interannual phenomenon similar to but weaker than the Pacific El Niño also occurs in the Atlantic, sometimes known as the Atlantic Niño (or the Atlantic equatorial mode). The warm events reach their maximum strength in the second half of the year, with manifestations focused primarily near the equator (e.g., Zebiak 1993; Carton and Huang 1994; Latif and Grotzner 2000; Wang 2002b). During a warm phase, trade winds in the equatorial western Atlantic are weak and SST is high in the equatorial eastern Atlantic. The reverse occurs during a cold phase. The Atlantic Niño is mostly independent of the Pacific ENSO variability; it has a shorter characteristic time scale and is not to be confused with the tropical Atlantic response to the Pacific ENSO.

The Atlantic also displays tropical Atlantic meridional gradient variability that results from the contrasting behaviors of SST in the tropical North Atlantic (TNA) and tropical South Atlantic (TSA), respectively. Some researchers have claimed that this behavior is a characteristic, antisymmetric "dipole" mode (e.g., Weare 1977; Hastenrath 1978; Moura and Shukla 1981; Servain 1991; Nobre and Shukla 1996; Chang et al. 1997; Xie 1999), while studies such as Houghton and Tourre (1992), Enfield and Mayer (1997), Mehta (1998), Enfield et al. (1999), Dommenget and Latif (2000), Wang (2002b), and Melice and Servain (2003) show that the TNA and TSA SST fluctuations vary independently and have fundamentally different time scales. Whatever the case, the tropical Atlantic meridional gradient variability, defined by the SST anomaly difference between the TNA and TSA, is correlated with north-south displacements of the Atlantic Intertropical Convergence Zone (ITCZ) and with strong climate anomalies over the surrounding land regions.

The tropical Western Hemisphere warm pool (WHWP), defined by Wang and Enfield (2001) as the ocean region covered by water

warmer than 28.5°C, is composed of the eastern North Pacific west of Central America; the Intra-Americas Sea (IAS), i.e., the Gulf of Mexico and the Caribbean; and the western tropical North Atlantic (see also Wang and Enfield 2003). The WHWP is the second largest tropical warm pool on earth. Unlike the Eastern Hemisphere warm pool in the western Pacific, which straddles the equator, the WHWP is entirely north of the equator. The WHWP has a large seasonal cycle and the interannual fluctuations of its areal extent are comparable to the annual variation, although it does not undergo large anomalous zonal excursions such as occur in the western Pacific. The WHWP is a critical component of the boreal summer climate of the Caribbean and surrounding land areas and also appears to influence the tropical and subtropical southeast Pacific (Wang and Enfield 2003).

Another important Atlantic climate phenomenon is the North Atlantic Oscillation (e.g., Hurrell 1995, 1996). Much of the climate variability over the North Atlantic and surrounding continents has been correlated with changes in the intensity of the NAO. The NAO is associated with the variations of surface westerly wind in the middle and high latitudes of the North Atlantic. It is characterized by a surface pressure seesaw between the Icelandic low and the subtropical anticyclone centered near the Azores. The SST signature obtained by correlating SST with the NAO (Azores minus Iceland) SLP index is a characteristic tripole pattern in the North Atlantic, while lacking significance in the South Atlantic.

This chapter reviews and examines climate phenomena of the Pacific ENSO, the Atlantic Niño, the tropical Atlantic meridional gradient variability, the WHWP, and the NAO and their associated regional atmospheric circulations. The rest of the chapter is organized as follows. Section 2 introduces the data used in the chapter. Section 3 shows the annual variability of the atmospheric circulation patterns over the Pacific and Atlantic. Sections 4, 5, 6, and 7 document atmospheric circulations associated with ENSO, the Atlantic Niño, the tropical Atlantic meridional gradient variability, and the NAO, respectively. Section 8 discusses the Walker and Hadley circulations that serve as a tropospheric bridge, transferring the Pacific ENSO effects to the Atlantic sector. Section 9 provides a summary and discussion.

2. DATA

The major data sources in this study are the NCEP/NCAR reanalysis field and the NCEP SST from January 1950 to December 1999. The NCEP/NCAR reanalysis field uses a state-of-the-art global data assimilation system on a 2.5° latitude by 2.5° longitude grid (see

Kalnay et al. [1996] for details). Variables used in this study are monthly SLP and monthly atmospheric horizontal wind velocity, vertical velocity, and velocity potential at levels of 1,000 mb, 925 mb, 850 mb, 700 mb, 600 mb, 500 mb, 400 mb, 300 mb, 250 mb, 200 mb, 150 mb, and 100 mb. The vertical component of the wind field in the reanalysis field is pressure vertical velocity. We multiply the pressure vertical velocity by –1, so positive values of the vertical velocity indicate an upward movement of air parcels.

Horizontal wind velocity can be divided into a nondivergent (or rotational) part and a divergent (or irrotational) part (e.g., Mancuso 1967; Krishnamurti 1971; Krishnamurti et al. 1973):

$$\vec{v} = \vec{v}_{\psi} + \vec{v}_{\chi} = \vec{k} \times \nabla\psi + \nabla\chi,$$

where ψ is stream function and χ is velocity potential. The first part does not contribute to atmospheric divergent fields associated with atmospheric vertical motion (it is nondivergent). It is well known that the Walker and Hadley circulations are thermally driven, associated with geographical foci of atmospheric convergence and divergence. In the tropics, atmospheric heating associated with convection induces atmospheric convergence and divergence that drive atmospheric vertical motion and circulation. This direct circulation, comprised of zonal (Walker) and meridional (Hadley) circulations, is therefore best characterized by the divergent component of flow and vertical motion. We will focus mainly on the distributions of atmospheric vertical motion and the divergent component of the wind when we discuss atmospheric circulations.

Monthly SST data are also used in this study. SST data are taken from the NCEP SST data set on a 2° latitude by 2° longitude grid from January 1950 through December 1999. These SST fields were produced by using a spatial interpolation method employing empirical orthogonal function analysis (see Smith et al. [1996] for the detailed description). With all of these data, we first calculate monthly climatologies based on the full record period (1950–99) and then anomalies are obtained by subtracting the monthly climatologies for each data set from the data.

3. ANNUAL VARIABILITY

Before we show anomaly variations of atmospheric circulations associated with ENSO and Atlantic climate variability, we first examine the seasonal cycle of tropospheric circulation patterns over the Pacific and Atlantic. Figure 6-1 shows the boreal winter (January) climatologies of tropospheric circulation. Centers of low (high) velocity potential are associated with divergent outflow (convergent inflow) winds. Notice that

divergence (convergence) in the upper troposphere corresponds to convergence (divergence) in the lower troposphere (e.g., Wang 2002a, b); however, we only show velocity potential and divergent wind in the upper troposphere of 200 mb in this chapter. Figures 6-1a and b show that centers of upper tropospheric divergence over the western Pacific, the Amazon, and tropical Africa are characterized by middle tropospheric upward motions. These patterns are manifestations of, or are consistent with, three of the known major global heat sources over the "maritime continent" of the western Pacific, the Amazon, and tropical Africa. The equatorial eastern Pacific and Atlantic are associated with upper tropospheric convergence and middle tropospheric downward vertical motion. All of these are consistent with the features of warm water in the western Pacific and western Atlantic, and the equatorial cold tongue in the eastern Pacific and eastern Atlantic.

Figure 6-1b shows manifestation of the Intertropical Convergence Zone in the Pacific and Atlantic—in particular, a narrow band of middle tropospheric upward vertical motion in the eastern Pacific around 10°N. The South Pacific Convergence Zone is also indicated around 10°S near the date line. An east-west band of downward motion in the middle troposphere along 20°N manifests the subtropical high. In the mid-latitudes, upward vertical motion is in the central North Pacific and Atlantic, and downward motion is located in the east of Asia and in the United States. Figure 6-1c shows the east-west equatorial circulation: the Pacific and Atlantic Walker circulations. The air ascends in the west, flows eastward in the upper troposphere, sinks in the east, and returns toward the west in the lower troposphere. For the Atlantic Walker circulation, the sinking and westward flows do not reach the lower troposphere during the boreal winter.

As is suggested by Figures 6-1a and b, the meridional circulations behave differently in different regions. Thus, we separately plot meridional-vertical circulations in the western Pacific, eastern Pacific, and Atlantic as shown in Figures 6-1d–f. In the western Pacific, the Hadley circulation shows the air rising in the tropical region, flowing poleward in the upper troposphere in both hemispheres, and returning to the tropics in the lower troposphere (Fig. 6-1d). In the eastern Pacific, the tropical circulation shows moist air rising in the ITCZ, then diverging northward and southward in the upper troposphere, and descending over the regions of the subtropical high and the equatorial cold tongue (Fig. 6-1e). The extratropics of the Northern Hemisphere (NH) shows the classical Ferrel circulation, with upward motion in the high latitudes and downward motion in the mid-latitudes (Fig. 6-1e). In the Atlantic, the meridional circulation shows both the Hadley circulation and the Ferrel circulation with upward motion near the equator (and south of the equator) and in the high latitudes, and downward motion in the northern subtropical Atlantic

(Fig. 6-1f). Figure 6-1 shows that the Pacific and Atlantic circulations are similar, except that the upward motion over land heat sources like South America is strongest near the ground, while the ascent over the ocean regions is strongest at higher levels.

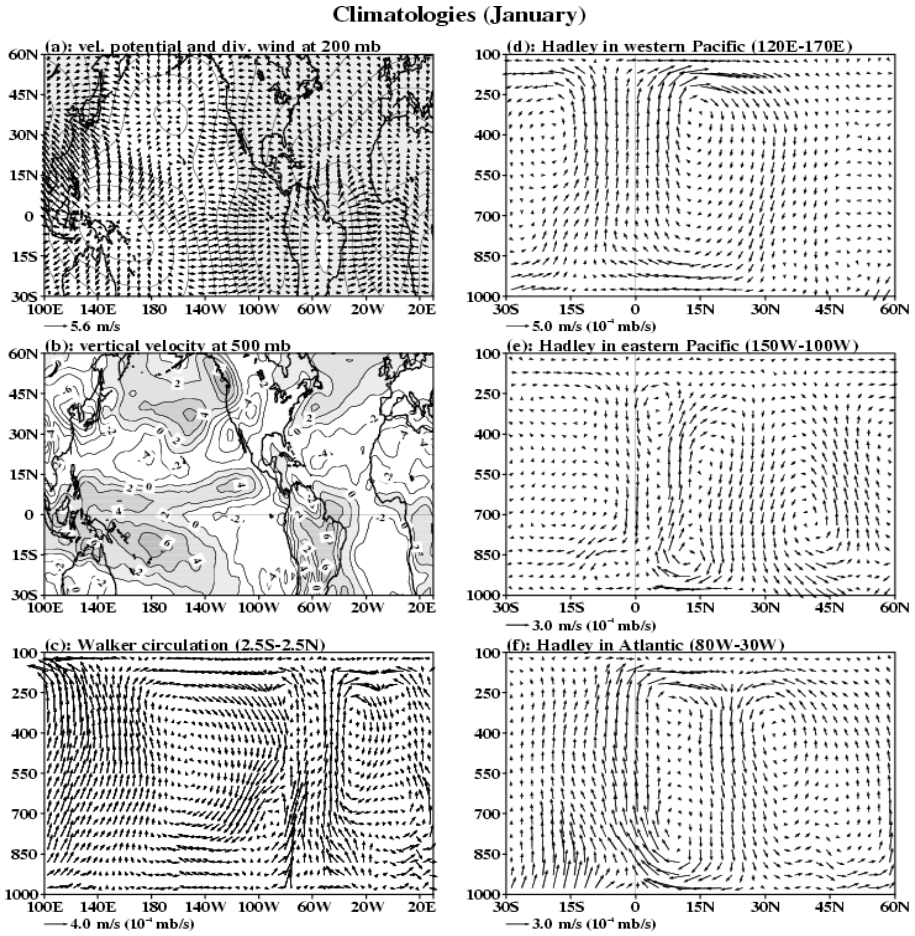

Figure 6-1. The boreal winter (January) climatologies of tropospheric circulation patterns. (a) 200 mb velocity potential (10^6 m^2/s) and divergent wind (m/s); (b) 500 mb vertical velocity (10^{-4} mb/s); (c) Walker circulation by averaging divergent wind and vertical velocity between 2.5°S and 2.5°N; (d) Hadley circulation in the western Pacific by averaging divergent wind and vertical velocity between 120°E and 170°E; (e) Hadley circulation in the eastern Pacific by averaging divergent wind and vertical velocity between 150°W and 100°W; and (f) Hadley circulation in the Atlantic by averaging divergent wind and vertical velocity between 80°W and 30°W. The vertical velocity is taken to be the nega-

tive of the pressure vertical velocity in the reanalysis; i.e., positive values indicate an upward movement of air parcels. Positive values are shaded.

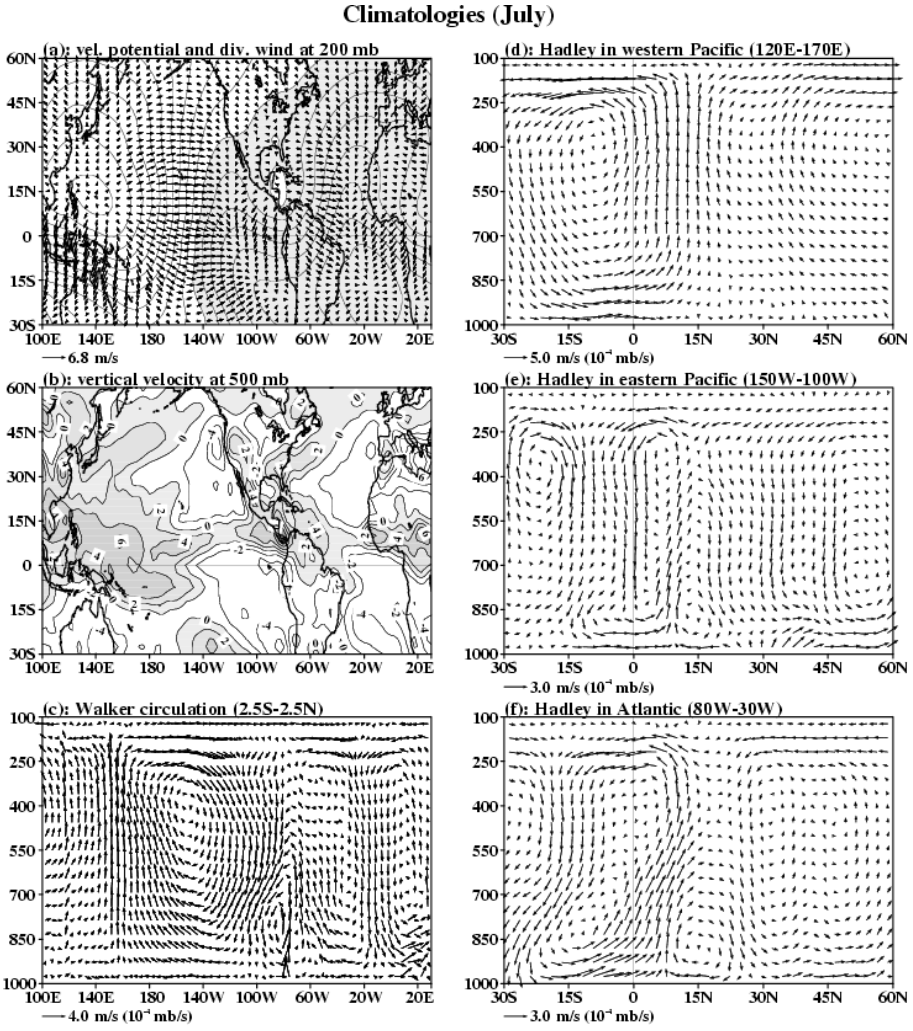

Figure 6-2. As in Fig. 6-1, but for the boreal summer (July).

The boreal summer (July) climatologies of tropospheric circulation are shown in Figure 6-2. The centers of upper tropospheric divergence associated with middle tropospheric ascent shift to the NH. For

example, the ascent over the Amazon (during the boreal winter) now shifts to the Intra-Americas Sea[1]. These shifts are associated with seasonal variability of the tropical Western Hemisphere warm pool that extends from the eastern North Pacific to the Gulf of Mexico, the Caribbean, and the western tropical North Atlantic (Wang and Enfield 2001, 2003). As was shown and discussed by Wang and Enfield (2001, 2003), the WHWP is dominated by SSTs in excess of 28.5°C and it is associated with eastern North Pacific and Atlantic hurricane activities and rainfall from northern South America to the southern tier of the United States. Figure 6-2c shows the Pacific and Atlantic zonal Walker circulations, with the strong ascent near the ground over the isthmus of Central America.

The Hadley circulation in the western Pacific shows a northward shift during the boreal summer, with a strong upward vertical motion north of the equator (Fig. 6-2d). The Atlantic Hadley circulation shows a downward motion over South America and an upward motion in the region of the WHWP enclosed by the 28.5°C SST (Wang and Enfield 2003), suggesting that the WHWP is a heating source of the summer Atlantic Hadley circulation (also Figs. 6-2a, b). All of the meridional circulations in Figures 6-2d–f show cross-equatorial flows from the Southern Hemisphere (SH) to the NH in the lower troposphere. It is also noteworthy that associated with the ascent over the region of the WHWP is the decent in the southeast Pacific (Fig. 6-2b), suggesting that the WHWP may link to the southeast Pacific. Figures 6-1 and 6-2 also show that the Hadley flows are always predominantly into the winter hemisphere.

4. ENSO

During 1950–99, there were seven most significant El Niño events (1957–58, 1965–66, 1972–73, 1982–83, 1986–87, 1991–92, and 1997–98) for which the SST anomalies in the NIÑO3 region (5°S–5°N, 150°W–90°W) exceeded 1°C (e.g., Wang 2002a). The maximum NIÑO3 SST anomalies for each warm event occurred during the calendar months from November to January except for the 1986–87 event, which had double peaks with the major one in the boreal summer. This result indicates a robust tendency for the mature phase of El Niño to occur toward the end of the calendar year (e.g., Rasmusson and Carpenter 1982). In order to understand the nature of atmospheric circulation patterns during El Niño, we calculate El Niño composites as shown

[1] The Intra-Americas Sea is broadly defined to include the Caribbean Sea, the Gulf of Mexico, the Florida-Bahamas area of the Atlantic Ocean, Bermuda and the northeast coast of South America (see Maul 1993).

in Figure 6-3 (from November of Niño year [0] to January of Niño year [+1]).

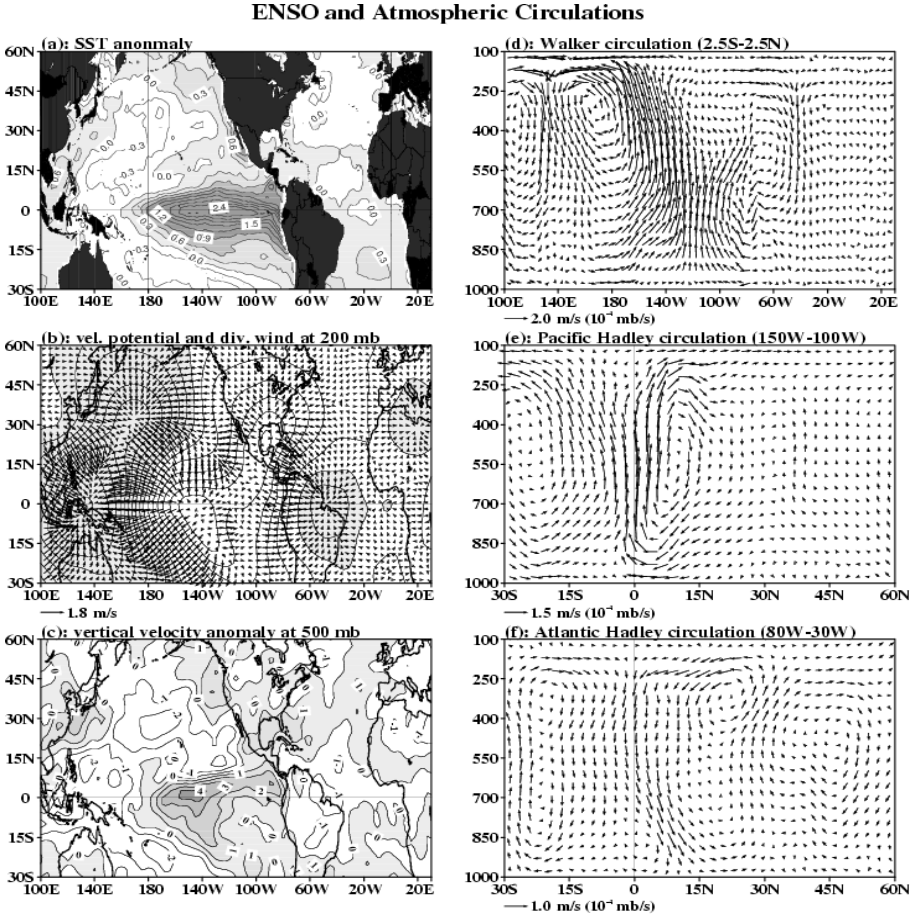

Figure 6-3. SST and atmospheric circulation anomaly composites during the mature phase of El Niño (November of Niño [0] to January of Niño [+1]). (a) SST anomalies; (b) 200 mb velocity potential anomalies (10^6 m^2/s) and divergent wind anomalies (m/s); (c) 500 mb vertical velocity anomalies (10^{-4} mb/s); (d) Walker circulation anomalies by averaging divergent wind and vertical velocity anomalies between 2.5°S and 2.5°N; (e) Hadley circulation anomalies in the eastern Pacific by averaging divergent wind and vertical velocity anomalies between 150°W and 100°W; (f) Hadley circulation anomalies in the Atlantic by averaging divergent wind and vertical velocity anomalies between 80°W and 30°W. The vertical velocity is taken to be the negative of the pressure vertical velocity in the reanalysis; i.e., positive values indicate an upward movement of air parcels. Positive values are shaded.

In the mature phase of El Niño, the equatorial eastern Pacific shows maximum anomalous warming, whereas the off-equatorial western Pacific and the central North Pacific show cold SST anomalies (Fig. 6-3a). Warm SST anomalies are found along the east coast of Asia and the west coast of North America. The TNA and WHWP also start to warm up and will reach their peaks during the spring and summer (e.g., Enfield and Mayer 1997; Wang and Enfield 2001, 2003). Upper tropospheric velocity potential anomalies show three centers near the equator: in the far equatorial western Pacific, the equatorial eastern Pacific, and the equatorial Atlantic; and three centers in the mid-latitudes: in the northwest Pacific, near Mexico, and overEurope (Fig. 6-3b). Associated with these divergent and convergent centers are middle tropospheric anomalous vertical motions (Fig. 6-3c). The equatorial eastern Pacific shows anomalous ascending motion, whereas the tropical western Pacific and the tropical Atlantic display anomalous descending motions. Anomalous descending motion is in the central North Pacific, and anomalous ascending motions are near the east coast of Asia and in the west coast of North America and over the United States.

The anomalous Walker circulation shows the air rising in the equatorial eastern Pacific, flowing westward and eastward aloft, sinking in the equatorial western Pacific and the equatorial Atlantic, and returning back to the eastern Pacific in the lower troposphere (Fig. 6-3d). Comparison of Figures 6-3c, d with Figures 6-1b, c shows that the Pacific and Atlantic Walker circulations are weakened during El Niño. The anomalous Hadley circulation in the eastern Pacific shows the air rising in the tropical region, flowing northward in the upper troposphere, descending in the mid-latitudes, and returning to the tropics in the lower troposphere (Fig. 6-3e). Notice that the anomalous Hadley circulation in the western Pacific has an opposite rotation to that of the anomalous Hadley circulation in the eastern Pacific (not shown; see Wang 2002a). The anomalous Hadley circulation in the Atlantic displays descending motion in the western equatorial Atlantic and eastern South America, and ascending motion in the subtropical North Atlantic and over subtropical South America (Figs. 6-3c and f).

Indices of the Pacific Walker circulation, the Hadley circulation in the eastern Pacific, the Hadley circulation in the western Pacific, and the Hadley circulation in the Atlantic (defined in the figure caption) are compared with the NIÑO3 SST anomalies, as shown in Figure 6-4. As is explained in the figure caption, these indices are defined based on the El Niño composite patterns in Figure 6-3. Variations of these circulations are evident in every El Niño/La Niña event.

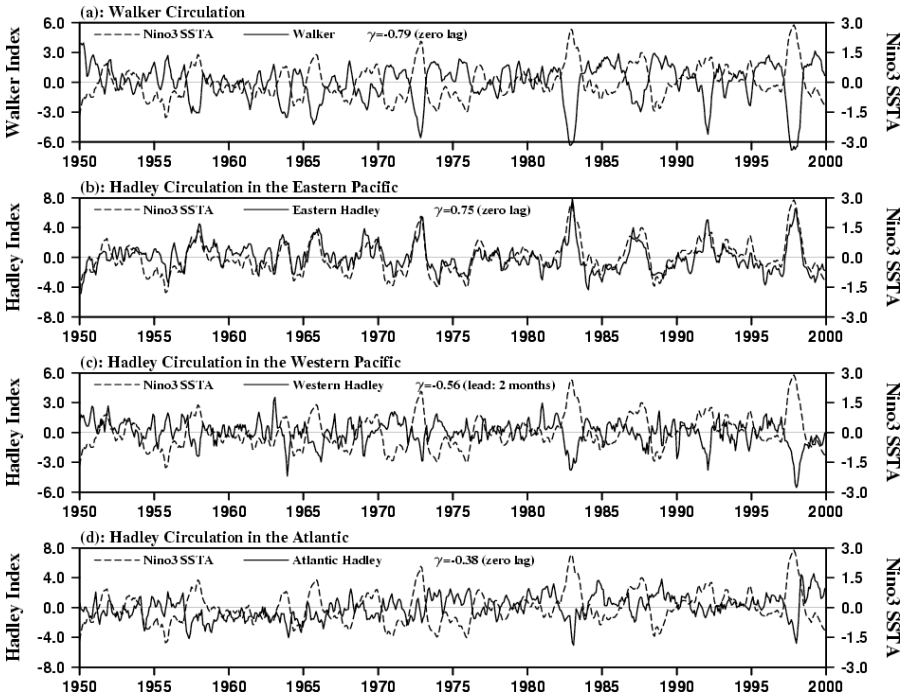

Figure 6-4. Comparison of the NIÑO3 SST anomalies with (a) the Walker circulation index; (b) the eastern Pacific Hadley circulation index; (c) the western Pacific Hadley circulation index; and (d) the Atlantic Hadley circulation index. The Walker index is defined by 500 mb vertical velocity anomaly difference between the equatorial eastern Pacific (5°S–5°N, 160°W–120°W) and the equatorial western Pacific (5°S–5°N, 120°E–160°E). The eastern Pacific Hadley index is defined by 500 mb vertical velocity anomaly difference between the central North Pacific (25°N–35°N, 170°E–150°W) and the equatorial eastern Pacific (5°S–5°N, 160°W–120°W). The western Pacific Hadley index is defined by 500 mb vertical velocity anomaly difference between the western North Pacific (25°N–35°N, 110°E–150°E) and the equatorial western Pacific (5°S–5°N, 120°E–160°E). The Atlantic Hadley index is defined by 500 mb vertical velocity anomaly difference between the tropical North Atlantic (20°N–30°N, 90°W–70°W) and the equatorial Atlantic (5°S–5°N, 50°W–30°W). All of the time series are 3-month running means. The value γ represents correlation coefficient.

The maximum correlations of the Pacific Walker circulation and the eastern Pacific Hadley circulation with the NIÑO3 SST anomalies are –0.79 and 0.75, respectively at zero lag. For the western Pacific Hadley circulation, the maximum correlation is –0.56, with the NIÑO3 SST anomalies leading the Hadley index by 2 months. The maximum correlation of the Atlantic Hadley circulation with the NIÑO3 SST anomalies is

–0.38 (above 95% significant level) at zero lag. Thus, during the warm phase of ENSO, the Pacific Walker circulation, the western Pacific Hadley circulation, and the Atlantic Hadley circulation are weakened, whereas the eastern Pacific Hadley circulation is strengthened. Weakening and strengthening of these circulations are manifestations of atmospheric responses to heating sources during ENSO (Figs. 6-3a, c).

From Figures 6-3 and 6-4, three points or comments can be mentioned. First, the higher (lower) correlation of the eastern Pacific (Atlantic) Hadley circulation with the NIÑO3 SST anomalies is due to the fact that NIÑO3 is a direct reflection of the heating anomalies in the Pacific, whereas it is only a teleconnected (indirect) proxy for the Atlantic. Second, the lower correlation of the Atlantic Hadley circulation with the NIÑO3 SST anomalies suggests that local heating anomalies also may be responsible for the Atlantic Hadley circulation. That is, the heating anomalies in the tropical Atlantic may also contribute to the Atlantic Hadley circulation (see next section for a discussion of the correlation between the Atlantic Hadley circulation and the ATL3 SST index—this index is defined as the mean sea surface temperature anomalies in the region 3°S–3°N, 20°W–0°). Third, the Amazon heating, which is a continental heat source in the boreal winter, not a maritime heating source, may also relate to the Atlantic Hadley circulation. The Atlantic Hadley circulation responds to the Amazon heating anomalies, which in turn are affected by ENSO and Atlantic climate variability.

5. THE ATLANTIC NIÑO

As is discussed by Zebiak (1993), Carton and Huang (1994), and Latif and Grotzner (2000), an interannual phenomenon similar to but weaker and more frequent than the Pacific El Niño also occurs in the Atlantic. During the Atlantic Niño, the largest near-equatorial SST anomalies are in the equatorial eastern Atlantic. Wang (2002b) showed that, during the 50-year period 1950–99 there were 11 significant warm events in which the ATL3 SST anomalies exceeded 0.7°C and lasted more than 1 month. The maximum ATL3 SST anomalies for these 11 warm events were centered in July 1963, July 1968, January 1973, November 1981, August 1984, August 1987, July 1988, June 1995, July 1996, January 1998, and July 1999. Among these 11 warm events, the peak phase of the ATL3 SST anomalies occurred in the boreal summer for 8 events and in the boreal winter for 3 events.

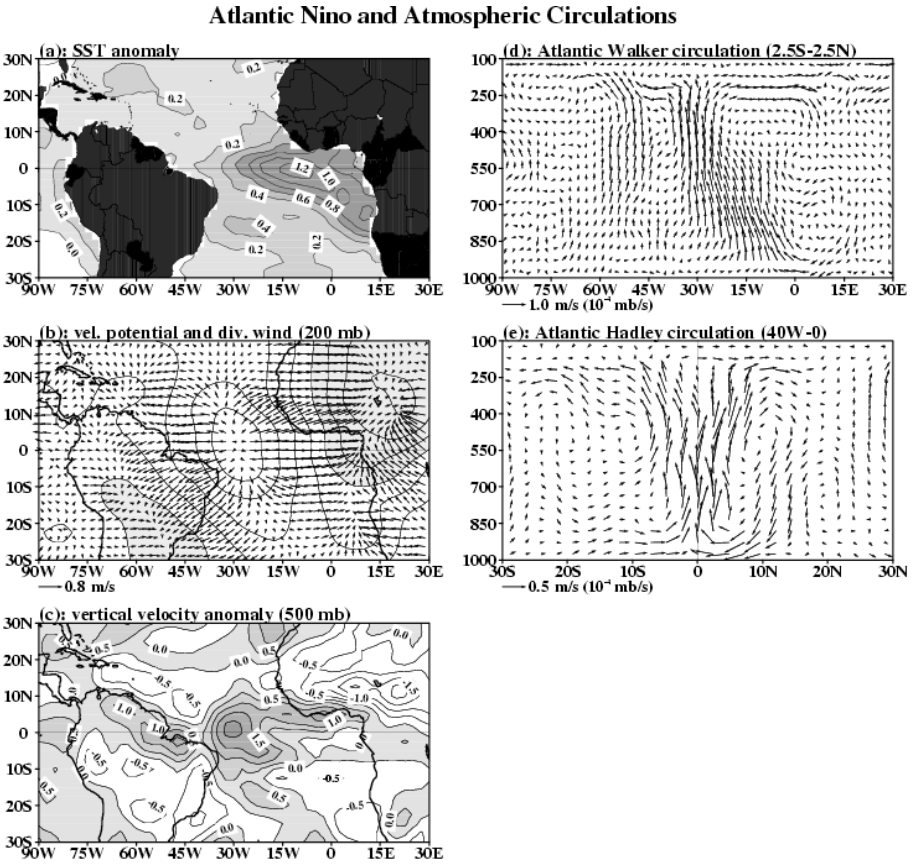

Figure 6-5. SST and atmospheric circulation anomaly composites during the peak phase of the Atlantic Niño. (a) SST anomalies; (b) 200 mb velocity potential anomalies (10^6 m^2/s) and divergent wind anomalies (m/s); (c) 500 mb vertical velocity anomalies (10^{-4} mb/s); (d) Atlantic Walker circulation anomalies by averaging divergent wind and vertical velocity anomalies between 2.5°S and 2.5°N; and (e) Atlantic Hadley circulation anomalies in the Atlantic by averaging divergent wind and vertical velocity anomalies between 40°W and 0°. The vertical velocity is taken to be the negative of the pressure vertical velocity in the reanalysis; i.e., positive values indicate an upward movement of air parcels. Positive values are shaded.

Atmospheric circulation patterns associated with the Atlantic Niño can be examined by compositing the 11 warm events mentioned above. Figure 6-5 shows the distribution of SST anomalies and atmospheric circulation anomalies during the peak phase of the Atlantic Niño. The entire tropical and subtropical Atlantic show positive SST anomalies, with maximum SST anomalies confined to the equatorial eastern

Atlantic (Fig. 6-5a). The upper tropospheric anomalous divergent outflow is in the tropical western Atlantic. The equatorial eastern Atlantic, specifically, the Gulf of Guinea, and the eastern tropical Africa land region show the upper tropospheric anomalous convergent inflow (Fig. 6-5b). Associated with these anomalous divergent/convergent flow fields are middle tropospheric anomalous ascending motion near the region of the equatorial Atlantic, and anomalous descending motion in the subtropics along 15°N (Fig. 6-5c). The equatorial zonal circulation shows anomalous ascending motion in the equatorial western Atlantic (Fig. 6-5d) near 30°W, whereas the associated ascending motion in the lower troposphere is skewed eastward to about 10°W. Although Figure 6-5d does not seem to show a clear anomalous zonal cell, we know that the Atlantic Walker circulation is weakened and extended eastward during the peak phase of the Atlantic Niño if we consider the mean state of the Atlantic Walker circulation in Figure 6-2c. The anomalous Hadley circulation shows ascent near the equator and descent in the subtropical region near 15°N. Thus, corresponding to the Atlantic Niño is a weakening of the Atlantic Walker circulation and a strengthening of the Atlantic Hadley circulation (Figs. 6-2a, b and Figs. 6-5b, c).

The indices of the Atlantic Walker circulation and the Atlantic Hadley circulation (defined in the figure caption) are shown in Figure 6-6 for comparison with the time series of the ATL3 SST anomalies that measures variability of the Atlantic Niño. Both the Atlantic Walker and Hadley circulations show high correlations with the ATL3 SST anomalies (–0.66 and 0.67, respectively). The ATL3 SST anomalies lead the Atlantic Walker index by 1 month, suggesting a response of the Walker circulation to warming in the equatorial eastern Atlantic. The Atlantic Niño is associated with a weakening of the Atlantic Walker circulation and a strengthening of the Atlantic Hadley circulation. This feature is similar to the relationship between the Pacific El Niño and the Pacific Walker and Hadley circulations, which is a key of the positive ocean-atmosphere feedback noted by Bjerknes (1969) for ENSO. During the Atlantic Niño, ascending motion associated with the IAS-Amazon heat source extends eastward. This eastward extension weakens the Atlantic Walker circulation and thus decreases surface equatorial easterly wind in the western Atlantic, which further increases SST in the equatorial eastern Atlantic. Thus, the positive ocean-atmosphere interaction associated with the Pacific Walker circulation, being responsible for the Pacific El Niño, is also operating in the Atlantic. However, in nature, both local air-sea coupling and the remote forcing may play a role in the Atlantic SST anomalies (e.g., Servain et al. 1982; Latif and Grotzner 2000).

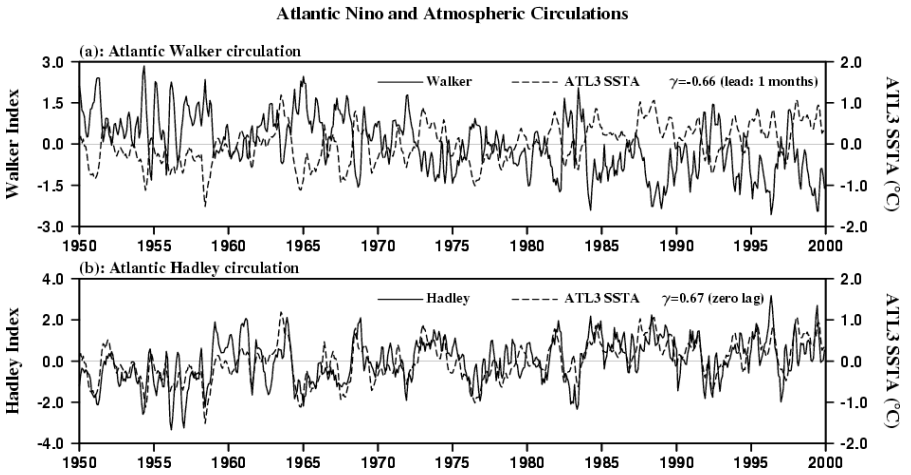

Figure 6-6. Comparisons of the ATL3 SST anomalies with (a) the Atlantic Walker circulation index and (b) the Atlantic Hadley circulation index. The Atlantic Walker index is defined by 500 mb vertical velocity anomalies in the region of 2.5°S–2.5°N, 40°W–20°W. The Atlantic Hadley index is defined by 500 mb vertical velocity anomaly difference between the regions of 12.5°N–17.5°N, 40°W–0° and 2.5°S–2.5°N, 40°W–0°. All of the time series are 3-month running means. The γ represents correlation coefficient.

6. THE TROPICAL ATLANTIC MERIDIONAL GRADIENT VARIABILITY

Many studies have investigated the tropical Atlantic meridional gradient variability (e.g., Moura and Shukla 1981; Folland et al. 1986; Servain 1991; Nobre and Shukla 1996; Rajagopalan et al. 1998; Xie and Tanimoto 1998; Enfield et al. 1999; Wang 2002b). Wang (2002b) defines a tropical North Atlantic index (5°N–25°N, 55°W–15°W) and a tropical South Atlantic index (0°–20°S, 30°W–10°E), and calculates the SST anomaly difference between the TNA and TSA regions to measure the tropical Atlantic meridional gradient variability. The main feature of the meridional (or interhemispheric) SST gradient variability is a slow variation on a decadal time scale. The decadal phases in the TNA-TSA time series are mainly due to the phased interaction between the separate and unrelated decadal variations of TNA and TSA, each with a different time scale. The meridional SST gradient is mainly positive for the periods of pre-1970, 1976–83, and after 1990 but prevailingly negative during 1971–75 and 1984–89.

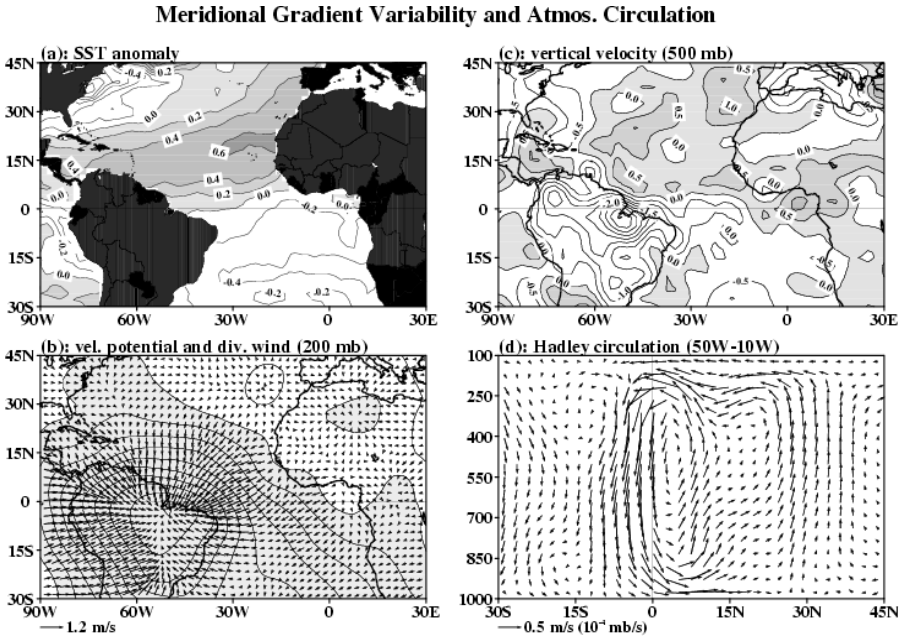

Figure 6-7. SST and atmospheric circulation anomalies for the tropical Atlantic meridional gradient variability. (a) SST anomalies; (b) 200 mb velocity potential and divergent wind anomalies; (c) 500 mb vertical velocity anomalies; and (d) Hadley circulation anomalies by averaging divergent wind and vertical velocity anomalies between 50°W and 10°W. The structures are calculated by the anomaly difference between the positive phase period of 1966–70 and the negative phase period of 1971–75. Positive values are shaded.

The structures of SST anomalies and atmospheric circulation anomalies for the meridional gradient variability can be seen by calculating the anomaly difference between a positive phase and a negative phase. Figure 6-7 shows the anomaly difference between the positive period of 1966–70 and the negative period of 1971–75. The tropical Atlantic SST anomalies show opposite signs: the TNA is warm and the TSA is cold, with the TNA being stronger than the TSA (Fig. 6-7a). The upper troposphere shows anomalous convergent inflow in the equatorial region and anomalous divergent outflow in the TNA and middle latitudes (Fig. 6-7b). Correspondingly, the middle troposphere is associated with anomalous descending motion in the TSA and over the Amazon, and anomalous ascending motion in the TNA and in the middle latitudes (Fig. 6-7c). The meridional anomalous circulation shows that the air rises over the TNA warm waters, diverges southward aloft, converges in the upper

troposphere to feed the strong subsidence in the equatorial TSA, then crosses the equator toward the TNA in the lower troposphere (Fig. 6-7d).

The time series of the Atlantic Hadley circulation index (defined in the figure caption) associated with the tropical Atlantic meridional gradient variability are shown in Figure 6-8. The maximum correlation of the Hadley circulation index with the meridional SST gradient variability is 0.59 (above the 99% significance level) when the meridional SST gradient variability lags the Hadley circulation by 1 month. Thus, the tropical Atlantic meridional gradient variability is associated with the variations of the Atlantic Hadley circulation.

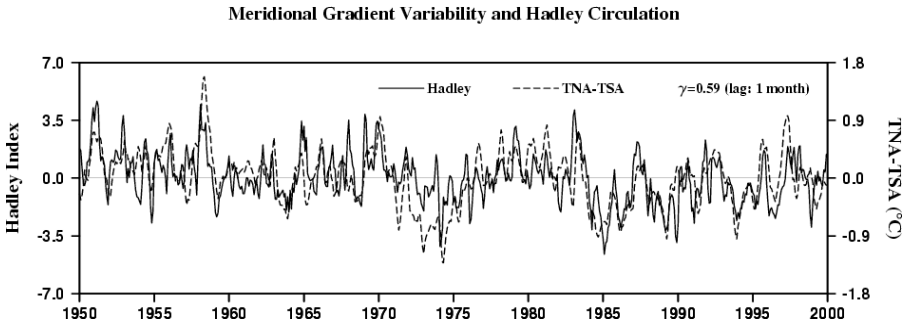

Figure 6-8. Comparisons of the tropical Atlantic meridional SST gradient with the Atlantic Hadley circulation index. The Hadley index is defined by 500 mb vertical velocity anomaly difference between the regions of 2.5°S–7.5°S, 40°W–20°W, and 25°N–30°N, 40°W–20°W. The meridional gradient mode is defined by the SST anomaly difference between the tropical North Atlantic region (5°N–25°N, 55°W–15°W) and the tropical South Atlantic region (0°–20°S, 30°W–10°E). All of the time series are 3-month running means. The γ represents correlation coefficient.

As was discussed in the Introduction, some studies have claimed that the tropical Atlantic meridional gradient variability is an antisymmetric "dipole" mode, while others show that the TNA and TSA vary independently and have different time scales. Therefore, we separately calculate the positive phase of 1966–70 and the negative phase of 1971–75. Although atmospheric circulation shows ascent over warm SST anomalies and descent over cold SST anomalies for either phase, there are differences between the positive and negative phases of the meridional gradient variability. For example, the upper tropospheric anomalous divergent outflow center for the negative phase of 1971–75 is further eastward in comparison with the anomalous convergent inflow center over the Amazon for the positive phase of 1966–70. For both the posi-

tive and negative phases, southern Africa shows middle tropospheric anomalous ascending motion. If the tropical Atlantic meridional gradient variability were an antisymmetric "dipole" mode, the tropospheric circulation patterns of the positive phase would be opposite to those of the negative phase. Our calculations thus do not seem to support an antisymmetric "dipole" mode of the tropical Atlantic meridional gradient variability.

7. THE NORTH ATLANTIC OSCILLATION

Another important climate phenomenon in the Atlantic is the NAO, whose positive phase is characterized by strong westerly air flow between the Icelandic low and the Azores high, particularly in winter. Hurrell (1995, 1996) defined an NAO index as the difference of winter (December–March) SLP anomalies between Lisbon, Portugal (38.43°N, 9.08°W) and Stykkishólmur, Iceland (65.06°N, 22.48°W). A striking feature of the NAO index has been the reversal from the negative index (weak meridional SLP gradient) to predominately positive index (high gradient) values starting near 1970. The winters of 1972–73, 1982–83, 1988–89, 1989–90, 1992–93, and 1994–95 are marked by high positive values of the NAO index.

The structures of SST and atmospheric variables for the high NAO index can be calculated by compositing anomalies of the 1972–73, 1982–83, 1988–89, 1989–90, 1992–93, and 1994–95 winters. Figure 6-9 shows the composites of SST and SLP anomalies, and anomalous atmospheric circulation patterns. The Atlantic Ocean shows an alternating pattern of zonally oriented positive-negative SST anomalies (Fig. 6-9a). The coolings appear in the North Atlantic and in the TNA. The warmings occur in the middle Atlantic with centers located at the east coast of the United States and the west coast of Europe, and in the TSA. However, the TSA SST anomalies do not significantly correlate with the NAO index (Visbeck et al. 1998; Wang 2002b). The reason for this difference (about the TSA) may be that the composite considers only the positive phase, whereas correlation deals with both the positive and negative phases.

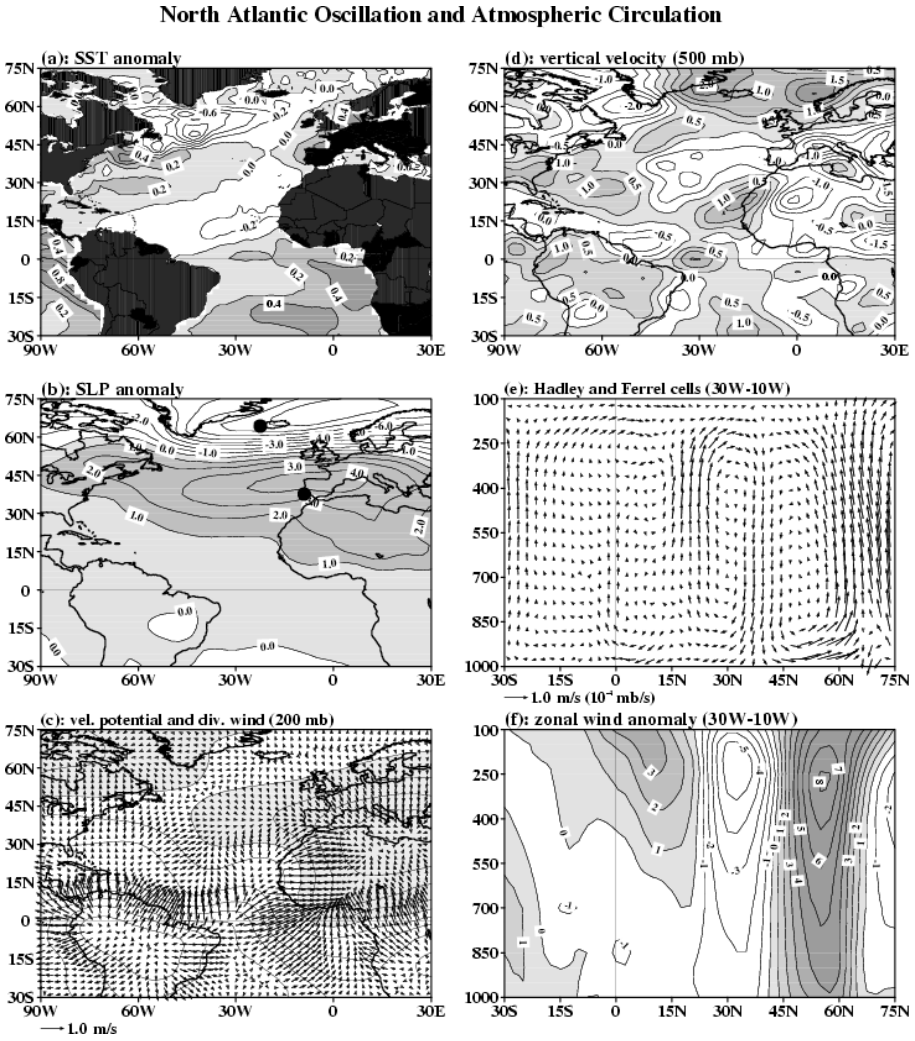

Figure 6-9. The structures of SST and atmospheric circulation anomalies for the high NAO index. (a) SST anomalies; (b) SLP anomalies; (c) 200 mb velocity potential and divergent wind anomalies; (d) 500 mb vertical velocity anomalies; (e) Atlantic Hadley and Ferrel circulation anomalies by averaging divergent wind and vertical velocity anomalies between 30°W and 10°W; and (f) zonal wind anomalies between 30°W and 10°W. The two dots in (b) are Lisbon, Portugal (38.43°N, 9.08°W) and Stykkishólmur, Iceland (65.06°N, 22.48°W), which are used to calculate the NAO index. Positive values are shaded.

Thus, in spite of seemingly being a quadrupole pattern, the spatial Atlantic SST pattern of the NAO is a tripole (e.g., Rodwell et al.

1999; Seager et al. 2000). The SLP anomalies simply show a meridional seesaw pattern, with low SLP anomalies in the high latitudes and high SLP anomalies south of about 55°N, including the Azores, which form the southern pole of the NAO index (Fig. 6-9b).

During periods when the NAO index is high, upper tropospheric anomalous divergent outflow centers are over the Amazon and the North Atlantic, whereas upper tropospheric anomalous convergent inflow centers are located in northern Africa and Europe and in the region of Greenland (Fig. 6-9c). Corresponding to these upper tropospheric anomalous divergent and convergent centers are the middle tropospheric anomalous ascending motion in the North Atlantic, in the southeast coast of the United States to the subtropical Atlantic, and over the Amazon, and anomalous descending motion in the region of Greenland and in Europe and Africa. The distribution of the vertical motion is consistent with the precipitation pattern of Hurrell et al. (2003) for high-low NAO index years (their Fig. 16). Drier conditions occur over much of Greenland, and much of central and southern Europe, the Mediterranean and parts of the Middle East, whereas more precipitation than normal falls from Iceland through Scandinavia and from the southeast coast of the United States to the subtropical Atlantic.

The anomalous meridional circulation shows a counterclockwise circulation in the North Atlantic and a clockwise circulation in the tropical-middle Atlantic (Fig. 6-9e). These two circulations correspond to the Ferrel cell and the Hadley cell, respectively. These anomalous circulations have the same rotations as the mean Ferrel and Hadley circulations, indicating that during the high NAO index periods, both the Ferrel and the Hadley circulations are strengthened. Zonal wind anomalies display westerly wind anomalies in the North Atlantic and easterly wind anomalies in the subtropical Atlantic (Fig. 6-9f), consistent with the strength of the Icelandic low and the Azores high during the high NAO index periods. These wind anomaly patterns extend through the whole troposphere, with the maximum zonal wind anomalies occurring in the upper troposphere. The distribution of the wind patterns seems to suggest that wind speed associated with latent heat flux is responsible for the SST anomaly patterns shown in Figure 6-9a (Visbeck et al. 2003; we will discuss it in Section 9).

The change of the wind and atmospheric circulations associated with the NAO can be further seen from the time series. Figure 6-10 shows a comparison of the NAO index with zonal wind anomalies in the North Atlantic, zonal wind anomalies in the middle to tropical Atlantic, the Ferrel circulation index, and the Hadley circulation index (defined in the figure caption). All of these indices are correlated with the NAO index. Every NAO event is associated with westerly wind anomalies between the Icelandic low and the Azores high, and easterly wind anomalies

south of the Azores high. Both the Ferrel circulation and the Hadley circulation are also closely related to the NAO index, suggesting that the meridional circulations may be important for the NAO.

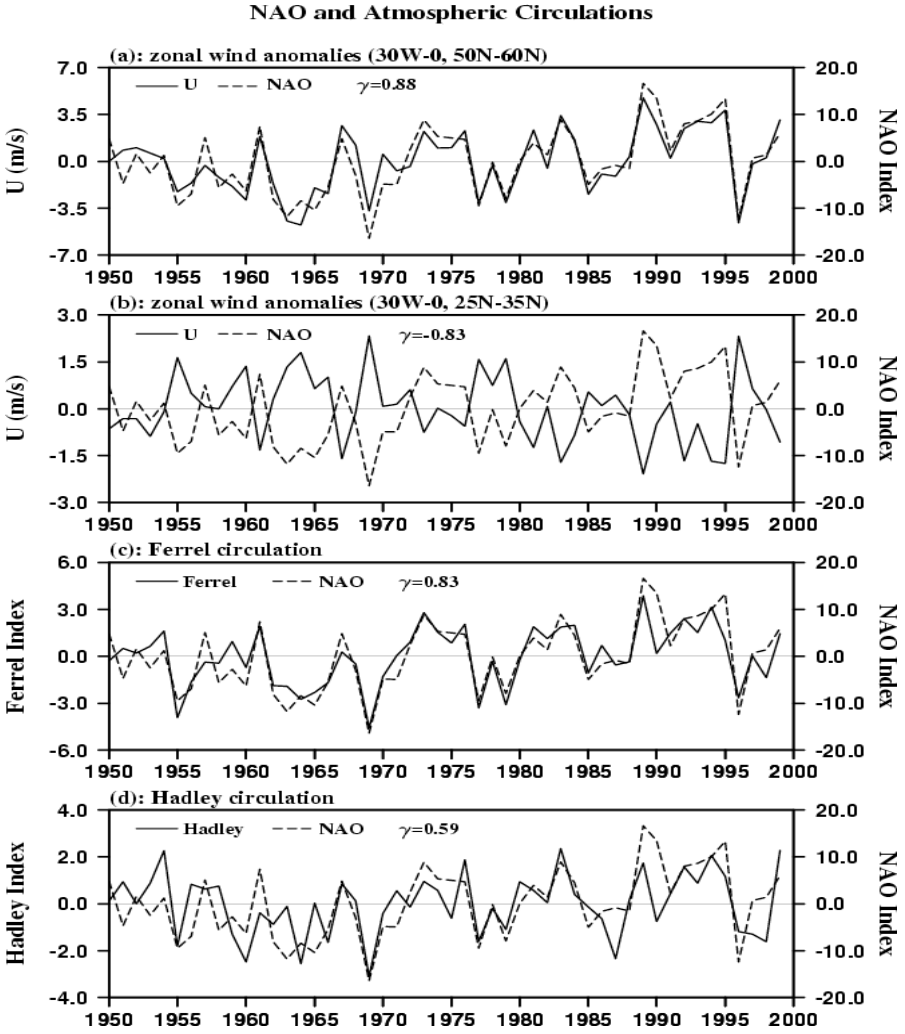

Figure 6-10. Comparisons of the NAO index with (a) 1,000 mb zonal wind anomalies in the North Atlantic of 50°N–60°N, 30°W–0°; (b) 1,000 mb zonal wind anomalies in the middle to tropical Atlantic of 25°N–35°N, 30°W–0°; (c) the Ferrel circulation index, and (d) the Hadley circulation index. The Ferrel index is defined by 500 mb vertical velocity anomaly difference between the regions of 35°N–40°N, 30°W–0°, and 60°N–65°N, 30°W–0°. The Hadley index is defined by 500 mb vertical velocity anomaly difference between the regions of 35°N–40°N, 30°W–0°, and 15°N–20°N, 30°W–0°. The NAO index is calculated

by the difference of winter (December–March) SLP anomalies between Lisbon, Portugal and Stykkishólmur, Iceland. The γ represents correlation coefficient at zero lag.

8. A TROPOSPHERIC BRIDGE FOR TRANSFERRING THE EFFECTS OF THE PACIFIC ENSO TO THE ATLANTIC SECTOR

Previous studies have shown that the TNA SST anomalies are related to the Pacific El Niño (e.g., Curtis and Hastenrath 1995; Enfield and Mayer 1997; Klein et al. 1999; Hastenrath 2000). The lagged cross-correlation between the TNA and NIÑO3 SST anomalies shows that the maximum positive correlation of 0.47 occurs when the TNA SST anomalies lag the NIÑO3 SST anomalies by 5 months (Wang 2002c). Recently, Wang (2002b, c) and Wang and Enfield (2003) showed that the Pacific ENSO variability is related to variations of the TNA and the WHWP. Wang and Enfield (2003) showed that during the 50-year period since 1950 there were five large warm pools, which on average reached their maximum anomaly in July. All warm pools occurred in the summer following recognized El Niño events and they also coincided with strong warming of the TNA. These warm pools were about twice as large as the climatological average for July (Fig. 6-11). Four of these large warm pools occurred in the boreal summer of Niño [+1] years (1958, 1983, 1987, 1998), consistent with Hastenrath et al. (1987) and Enfield and Mayer (1997). Note, however, that large warm pools did not follow four other recognized El Niño events (1966, 1973, 1977, 1992). The occurrence of Pacific El Niño is no guarantee of a large ensuing warm pool. Further studies are needed for understanding why extremely anomalous warm pools develop the year following certain Pacific El Niño events, but not others.

How does the Pacific El Niño affect the TNA and the WHWP in the Atlantic sector? There are two possible ways for the Pacific El Niño to affect the Atlantic sector: (1) through the Pacific–North American (PNA) pattern; and (2) through the Walker and Hadley circulations. Wallace and Gutzler (1981) and Horel and Wallace (1981) found that equatorial Pacific warming is accompanied by a teleconnection PNA pattern that shows alternating positive and negative geopotential height anomalies emanated from the Pacific, directed poleward, and curved eastward and then equatorward. It is possible that the Pacific El Niño affects the northern Atlantic subtropical high through the PNA pattern. Changes of the Atlantic subtropical high induce variations of the north-

east trade winds on its southern flank and then affect the TNA SST anomalies.

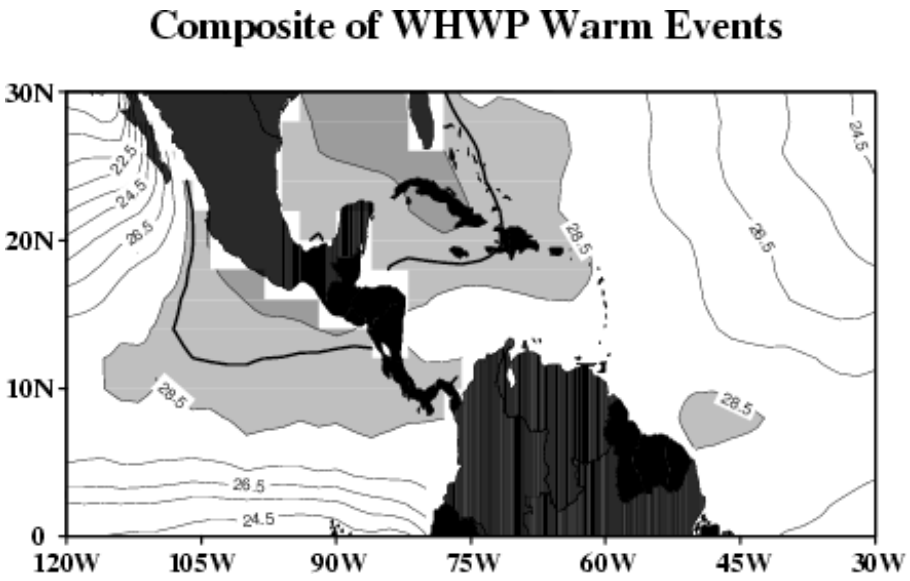

Figure 6-11. SST composites in July for the WHWP interannual warm events. The composites are calculated by averaging over the warm years of 1958, 1969, 1983, 1987, and 1998. The shading represents water warmer than 28.5°C. The dark contour is July climatological SST warmer than 28.5°C.

The Walker and Hadley circulations may also link the Pacific El Niño and warming in the tropical Atlantic. Pacific El Niño conditions were established during the winter seasons prior to warming of TNA and the WHWP. In Figure 6-3 we see composite-averaged maps of the velocity potential, divergent wind, vertical velocity, and circulation departures for the mature phase of El Niño. Most prominent are large convergent and divergent areas over northern South America and the Gulf of Mexico, respectively, at 200 mb (Fig. 6-3b). The upper convergence is fed by an anomalous northerly flow from the north, which in turn diverges from the Caribbean and subtropical North Atlantic. Figure 6-3d shows an anomalous zonal Walker circulation. The Atlantic Hadley circulation is weakened during the mature phase of the Pacific El Niño (Fig. 6-3f). Associated with these circulations are anomalous descending over northern South America and anomalous ascending motion in the region of the North Atlantic subtropical high-pressure system (Fig. 6-3c).

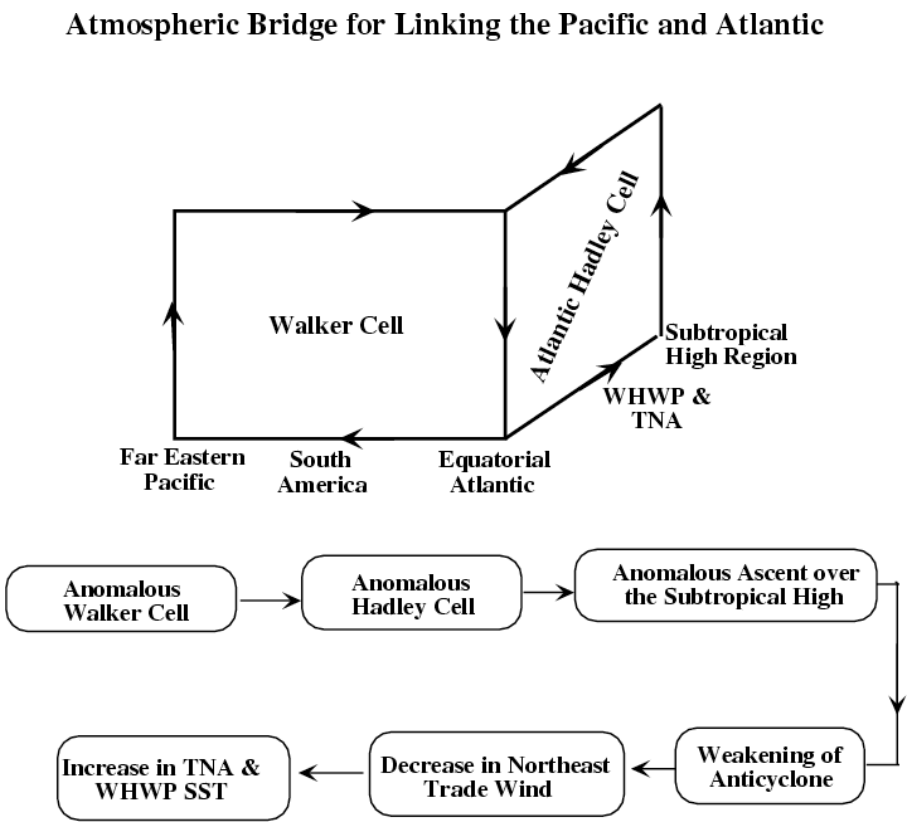

Figure 6-12. Schematic diagram showing linkage of the Pacific El Niño with the tropical North Atlantic and the Western Hemisphere warm pool by the Walker and Hadley circulations.

The connection associated with the Walker and Hadley circulations, seen from the data, is schematically summarized in Figure 6-12. The anomalous descending over northern South America is consistent with reduced rainfall observed over parts of Colombia, Venezuela, and northern Brazil (Ropelewski and Halpert 1987). The anomalous subtropical ascending motion corresponds to a late winter weakening of the North Atlantic anticyclone and the associated northeast (NE) trade winds over its southern limb in the TNA region. With the weaker NE trades come reduced evaporation and entrainment (from below the oceanic mixed layer) during late winter and early spring, leading to warmer SST anomalies over the TNA region by late spring and early summer (Enfield and Mayer 1997 and others). The TNA warming along 5°–15°N

extends well into the region of the Outer Antilles that by May sees SSTs above 27°C (Wang and Enfield 2003), required for large-scale tropical convection at the start of the Caribbean rainy season. Thus, the Walker and Hadley circulations can serve as a "tropospheric bridge" for transferring the Pacific El Niño SST anomalies to the Atlantic sector and inducing the TNA SST anomalies just at the time of year when the warm pool is developing.

9. SUMMARY AND DISCUSSION

There are three major localized tropical heat sources: (1) over the maritime continent of the western Pacific; (2) migrating between the Amazon and the Intra-Americas Sea; and (3) over tropical Africa. It is widely known that zonal excursion of the western Pacific heat source is associated with the Pacific ENSO phenomenon that affects climate variations on a global scale. The seasonally varying IAS-Amazon heat source affects climate from South to North America and tropical storms and hurricanes on both sides of Central America. The heat source moves seasonally, generally, being most north and west over the WHWP in the boreal summer, and south and east over northern South America in the boreal winter. Associated with the seasonal movements of the heat sources are the seasonal variations of the equatorial zonal Walker circulation, the tropical meridional Hadley circulation, and the extratropical meridional Ferrel circulation.

ENSO shifts the western Pacific heat source and atmospheric convective activity and then affects global atmospheric circulation. During El Niño, the equatorial Pacific Walker circulation is observed to be weakened. The anomalous meridional Hadley circulation in the eastern Pacific shows the air rising in the tropics, flowing poleward in the upper troposphere, sinking in the subtropics, and returning to the tropics in the lower troposphere. The anomalous Hadley circulation in the western Pacific is opposite to that in the eastern Pacific, indicating a weakening of the western Pacific Hadley circulation during El Niño. The NCAR/NCEP reanalysis field also shows that El Niño weakens the Atlantic Hadley circulation, consistent with an earlier result of Klein et al. (1999) that is inferred from correlation maps of satellite observations, and with the direct circulation analyses of Mestas-Nuñez and Enfield (2001) and Wang (2002a). Wang (2002b, c) and Wang and Enfield (2003) suggest that following El Niño winters in which the Atlantic Hadley circulation is strongly weakened, the decreased subsidence over the subtropical North Atlantic results in the late winter weakening of the NE trades off Africa, the associated spring TNA warming (Enfield and

Mayer 1997 and others), and the large summer warm pools (Wang and Enfield 2001).

The Atlantic Niño, similar to but weaker and more frequent than the Pacific El Niño and unrelated to it, shows positive SST anomalies in the equatorial eastern Atlantic. During the warm phase of the Atlantic Niño, ascending motion associated with the IAS-Amazon heat source extends eastward. This eastward extension weakens the Atlantic Walker circulation and thus decreases surface equatorial easterly wind in the western Atlantic, which in turn further increases SST in the equatorial eastern Atlantic. Thus, the positive ocean-atmosphere interaction associated with the Pacific Walker circulation, being responsible for the Pacific El Niño (Bjerknes 1969), seems to be also operating in the Atlantic. The Atlantic Hadley circulation is observed to be strengthened during the warm phase of the Atlantic Niño.

The Atlantic is unique in having the tropical meridional gradient variability, which has a strong impact on rainfall over surrounding land areas due to the associated migrations of the Atlantic ITCZ. The meridional gradient anomaly is significant either when the TNA is anomalous or when the TSA is anomalous or when both conditions exist nearly simultaneously and are opposite in sign. Corresponding to this meridional variability is an atmospheric meridional circulation in which the air rises over the warm SST anomaly region, flows toward the cold SST anomaly region aloft, converges in the upper troposphere to feed the strong subsidence and lower tropospheric divergence in the cold SST anomaly region, then crosses the equator toward the warm SST anomaly region in the lower troposphere. Since the lower tropospheric air always crosses the equator toward the warm SST anomalies, the Coriolis force will deflect air to the east (the west) over the warm (cold) SST anomaly regions. Tropical zonal wind anomalies are thus westerly (easterly) over the warm (cold) anomaly regions in the lower troposphere.

The SST pattern during the high NAO index periods shows a tripole, with cold SST anomalies in the northwest Atlantic and in the TNA and warm SST anomalies in the middle Atlantic. Accompanied by this SST anomaly pattern are a stronger Ferrel circulation and a stronger Hadley circulation. The zonal wind anomalies display westerly wind anomalies in the North Atlantic and easterly wind anomalies in the middle Atlantic, consistent with the strength of the Icelandic low and the Azores high during the high NAO index periods. The zonal wind anomaly distribution is also consistent with the strengthening of the meridional Ferrel and Hadley circulations. The strengthening of the Ferrel and Hadley circulations is associated with anomalous descending motion over the middle Atlantic. Near the sea surface, sinking air is divergent and flows both northward and southward as low branches of the Ferrel and Hadley circulations, respectively. The northward (southward) flowing air is de-

flected to the east (west) by the Coriolis force, resulting in westerly (easterly) wind anomalies in the North (middle) Atlantic. Since the mean zonal winds are westerly in the North and middle Atlantic, this zonal wind anomaly distribution increases (decreases) wind speed in the North (middle) Atlantic. The increasing (decreasing) of wind speed result in an increase (decrease) of latent heat flux that cools (warms) the North (middle) Atlantic (see Visbeck et al. [2003] for review). The TNA cooling when the NAO index is high (Fig. 6-9a) is also consistent with the zonal wind anomalies in the TNA (Fig. 6-9f). The negative values of the surface zonal wind anomalies in the TNA indicate the strength of the northeast trade winds, which will increase latent heat flux and then cool the TNA.

The Walker and Hadley circulations can serve as a "tropospheric bridge" for transferring the Pacific El Niño SST anomalies to the Atlantic sector and inducing the TNA SST anomalies just at the time of year when the warm pool is developing. As the Pacific El Niño warming culminates near the end of the calendar year, an alteration of the low-latitude direct circulation occurs, featuring (1) an anomalous weakening of the convection over northern South America, (2) Walker circulation anomalies along the equatorial strip to the east and west, and (3) a weakened northward Hadley flow aloft. The Hadley weakening results in less subsidence over the subtropical North Atlantic, an associated breakdown of the anticyclone, and a weakening of the NE trades in the TNA. The wind weakening leads to less evaporative surface cooling and entrainment of colder water from below the shallow mixed layer, resulting in positive SST anomalies. The TNA anomalies thus expand the WHWP area and increase the WHWP SST anomalies, just when warm pool development is taking place. The opposite is presumed to occur during boreal winters with unusually cool SSTs in the equatorial Pacific.

The Hadley circulation in some studies is referred to as a global zonal mean meridional circulation (e.g., Oort and Yienger 1996; Trenberth et al. 2000; and references there). Since ENSO is characterized as a strong east-west contrast phenomenon and this chapter focuses on atmospheric circulations associated with individual climate phenomena, we herein show the regional atmospheric circulations by using the atmospheric vertical velocity and the divergent component of wind. The divergent wind and vertical velocity also show a mid-latitude zonal circulation over the North Pacific (see Wang 2002a). However, we should keep in mind that the atmospheric circulations shown in this chapter may not be closed cells, in particular if we also consider the rotational component of wind.

10. ACKNOWLEDGMENTS.

This work was supported by a grant from the National Oceanic and Atmospheric Administration (NOAA) Office of Global Programs and by the NOAA Environmental Research Laboratories through their base funding of the Atlantic Oceanographic and Meteorological Laboratory. Discussions with and comments by Dave Enfield are appreciated. Two anonymous reviewers provided useful comments that helped improve the manuscript.

11. REFERENCES

Bjerknes, J. 1969. Atmospheric teleconnections from the equatorial Pacific. *Monthly Weather Review* 97: 163–172.

Carton, J.A., and B. Huang. 1994. Warm events in the tropical Atlantic. *Journal of Physical Oceanography* 24: 888–903.

Chang, P., L. Ji, and H. Li. 1997. A decadal climate variation in the tropical Atlantic Ocean from thermodynamic air-sea interactions. *Nature* 385: 516–518.

Curtis, S., and S. Hastenrath. 1995. Forcing of anomalous sea surface temperature evolution in the tropical Atlantic during Pacific warm events. *Journal of Geophysical Research* 100: 15835–15847.

Dommenget, D., and M. Latif. 2000. Interannual to decadal variability in the tropical Atlantic. *Journal of Climate* 13: 777–792.

Enfield, D.B., and D.A. Mayer. 1997. Tropical Atlantic sea surface temperature variability and its relation to El Niño-Southern Oscillation. *Journal of Geophysical Research* 102: 929–945.

Enfield, D.B., A.M. Mestas-Nuñez, D.A. Mayer, and L. Cid-Serrano. 1999. How ubiquitous is the dipole relationship in tropical Atlantic sea surface temperature? *Journal of Geophysical Research* 104: 7841–7848.

Folland, C.K., T.N. Palmer, and D.E. Parker. 1986. Sahel rainfall and worldwide sea temperatures, 1901–85. *Nature* 320: 602–607.

Hastenrath, S. 1978. On modes of tropical circulation and climate anomalies. *Journal of Atmospheric Science* 35: 2222–2231.

Hastenrath, S. 2000. Upper air mechanisms of the Southern Oscillation in the tropical Atlantic sector. *Journal of Geophysical Research* 105: 14997–15009.

Hastenrath, S., L.C. de Castro, and P. Aceituno. 1987. The Southern Oscillation in the Atlantic sector. *Contributions to Atmospheric Physics* 60: 447–463.

Horel, J.D., and J.M. Wallace. 1981. Planetary-scale atmospheric phenomena associated with the Southern Oscillation. *Monthly Weather Review* 109: 813–829.

Houghton, R.W., and Y. Tourre. 1992. Characteristics of low-frequency sea surface temperature fluctuations in the tropical Atlantic. *Journal of Climate* 5: 765–771.

Hurrell, J.W. 1995. Decadal trends in the North Atlantic Oscillation: Regional temperature and precipitation. *Science* 269: 676–679.

Hurrell, J.W. 1996. Influence of variations in extratropical wintertime teleconnections on Northern Hemisphere temperature. *Geophysical Research Letters* 23: 665–668.

Hurrell, J.W., Y. Kushnir, G. Ottersen, and M. Visbeck. 2003. An overview of the North Atlantic Oscillation. In, Hurrell, J.W., Y. Kushnir, G. Ottersen, and M. Visbeck

(eds.). *The North Atlantic Oscillation: Climatic Significance and Environmental Impact*. AGU Geophysical Monograph Series, pp. 1–35.

Kalnay, E., and Co-authors. 1996. The NCEP/NCAR 40-year reanalysis project. *Bulletin of the American Meteorological Society* 77: 437–471.

Klein, S.A., B.J. Soden, and N.C. Lau. 1999. Remote sea surface temperature variations during ENSO: Evidence for a tropical atmospheric bridge. *Journal of Climate* 12: 917–932.

Krishnamurti, T.N. 1971. Tropical east-west circulations during the northern summer. *Journal of Atmospheric Science* 28: 1342–1347.

Krishnamurti, T.N., M. Kanamitsu, W.J. Koss, and J.D. Lee. 1973. Tropical east-west circulations during the northern winter. *Journal of Atmospheric Science* 30: 780–787.

Latif, M., and A. Grotzner. 2000. The equatorial Atlantic oscillation and its response to ENSO. *Climate Dynamics* 16: 213–218.

Mancuso, R.L. 1967. A numerical procedure for computing fields of streamfunction and velocity potential. *Journal of Applied Meteorology* 6: 994–1001.

Maul, G.A. (Ed.) 1993. *Climatic Change in the Intra-Americas Sea*. UNEP. New York: Routledge, Chapman and Hall, 389 pp.

Mehta, V.M. 1998. Variability of the tropical ocean surface temperatures at decadal-multidecadal timescales. Part I: The Atlantic Ocean. *Journal of Climate* 11: 2351–2375.

Melice, J.-L., and J. Servain. 2003. The tropical Atlantic meridional SST gradient index and its relationships with the SOI, NAO and Southern Ocean. *Climate Dynamics* 20: 447–464.

Mestas-Nuñez, A.M., and D.B. Enfield. 2001. Eastern equatorial Pacific SST variability: ENSO and non-ENSO components and their climatic associations. *Journal of Climate* 14: 391–402.

Moura, A., and J. Shukla. 1981. On the dynamics of droughts in northeast Brazil: Observations, theory, and numerical experiments with a general circulation model. *Journal of Atmospheric Science* 38: 2653–2675.

Neelin, J.D., D.S. Battisti, A.C. Hirst, F.-F. Jin, Y. Wakata, T. Yamagata, and S.E. Zebiak. 1998. ENSO theory. *Journal of Geophysical Research* 103: 14262–14290.

Nobre, P., and J. Shukla. 1996. Variations of sea surface temperature, wind stress, and rainfall over the tropical Atlantic and South America. *Journal of Climate* 9: 2464–2479.

Oort, A.H., and J.J. Yienger. 1996. Observed interannual variability in the Hadley Circulation and its connection to ENSO. *Journal of Climate* 9: 2751–2767.

Philander, S.G. 1990. *El Niño, La Niña, and the Southern Oscillation*. London: Academic Press, 289 pp.

Rajagopalan, B., Y. Kushnir, and Y.M. Tourre. 1998. Observed decadal midlatitude and tropical Atlantic climate variability. *Geophysical Research Letters* 25: 3967–3970.

Rasmusson, E.M., and T.H. Carpenter. 1982. Variations in tropical sea surface temperature and surface wind fields associated with the Southern Oscillation/El Niño. *Monthly Weather Review* 110: 354–384.

Rodwell, M.J., D.P. Powell, and C.K. Folland. 1999. Oceanic forcing of the wintertime North Atlantic Oscillation and European climate. *Nature* 398: 320–323.

Ropelewski, C.F., and M.S. Halpert. 1987. Global and regional scale precipitation patterns associated with the El Niño/Southern Oscillation. *Monthly Weather Review* 115: 1606–1626.

Seager, R., Y. Kushnir, M. Visbeck, N. Naik, J. Miller, G. Karhmann, and H. Cullen. 2000. Causes of Atlantic Ocean climate variability between 1958 and 1998. *Journal of Climate* 13: 2845–2862.

Servain, J. 1991. Simple climatic indices for the tropical Atlantic Ocean and some applications. *Journal of Geophysical Research* 96: 15137–15146.

Servain, J., J. Picaut, and J. Merle. 1982. Evidence of remote forcing in the equatorial Atlantic Ocean. *Journal of Physical Oceanography* 12: 457–463.

Smith, T.M., R.W. Reynolds, R.E. Livezey, and D.C. Stokes. 1996. Reconstruction of historical sea surface temperature using empirical orthogonal functions. *Journal of Climate* 9: 1403–1420.

Trenberth, K.E., D.P. Stepaniak, and J.M. Caron. 2000. The global monsoon as seen through the divergent atmospheric circulation. *Journal of Climate* 13: 3969–3993.

Visbeck M., and Co-authors. 1998. Atlantic climate variability experiment prospectus. A consensus document of US and European scientists reflecting the findings of workshops in Lamont (September 1997), Dallas (February 1998), and Florence (May 1998), 49 pp.

Visbeck, M., E.P. Chassignet, R.G. Curry, T.L. Delworth, R.R. Dickson, and G. Krahmann. 2003. The ocean's response to North Atlantic Oscillation variability. In, Hurrell, J.W., Y. Kushnir, G. Ottersen, and M. Visbeck (eds.). *The North Atlantic Oscillation: Climatic Significance and Environmental Impact*. AGU Geophysical Monograph Series, pp. 113–145.

Wallace, J.M., and D.S. Gutzler. 1981. Teleconnections in the geopotential height field during the Northern Hemisphere winter. *Monthly Weather Review* 109: 784–812.

Wang, C. 2002a. Atmospheric circulation cells associated with the El Niño-Southern Oscillation. *Journal of Climate* 15: 399–419.

Wang, C. 2002b. Atlantic climate variability and its associated atmospheric circulation cells. *Journal of Climate* 15: 1516–1536.

Wang, C. 2002c. ENSO and atmospheric circulation cells. *CLIVAR Exchanges* 7: 9–11.

Wang, C., and D.B. Enfield. 2001. The tropical Western Hemisphere warm pool. *Geophysical Research Letters* 28: 1635–1638.

Wang, C., and D.B. Enfield. 2003. A further study of the tropical Western Hemisphere warm pool. *Journal of Climate* 16: 1476–1493.

Weare, B.C. 1977. Empirical orthogonal analysis of Atlantic Ocean surface temperatures. *Quarterly Journal of the Royal Meteorological Society* 103: 467–478.

Xie, S.P. 1999. A dynamic ocean-atmosphere model of the tropical Atlantic decadal variability. *Journal of Climate* 12: 64–70.

Xie, S.P., and Y. Tanimoto. 1998. A pan-Atlantic decadal climate oscillation. *Geophysical Research Letters* 25: 2185–2188.

Zebiak, S.E. 1993. Air-sea interaction in the equatorial Atlantic region. *Journal of Climate* 6: 1567–1586.